

On the Energy Efficiency of LT Codes in Proactive Wireless Sensor Networks

Jamshid Abouei[†], *Member, IEEE*, J. David Brown^{††}, Konstantinos N. Plataniotis[†], *Senior Member, IEEE* and
Subbarayan Pasupathy[†], *Life Fellow, IEEE*

[†] The Edward S. Rogers Sr. Dept. of Electrical and Computer Engineering,
University of Toronto, Toronto, Canada, Emails: {abouei, kostas, pas}@comm.utoronto.ca

^{††} Ottawa, Canada, Tel: 613-236-1051, Email: david.jw.brown@yahoo.com

Abstract

This paper presents the first in-depth analysis on the energy efficiency of LT codes with Non Coherent M-ary Frequency Shift Keying (NC-MFSK), known as *green modulation* [1], in a proactive Wireless Sensor Network (WSN) over Rayleigh flat-fading channels with path-loss. We describe the proactive system model according to a pre-determined time-based process utilized in practical sensor nodes. The present analysis is based on realistic parameters including the effect of channel bandwidth used in the IEEE 802.15.4 standard, and the active mode duration. A comprehensive analysis, supported by some simulation studies on the probability mass function of the LT code rate and coding gain, shows that among uncoded NC-MFSK and various classical channel coding schemes, the optimized LT coded NC-MFSK is the most energy-efficient scheme for distance d greater than the pre-determined threshold level d_T , where the optimization is performed over coding and modulation parameters. In addition, although uncoded NC-MFSK outperforms coded schemes for $d < d_T$, the energy gap between LT coded and uncoded NC-MFSK is negligible for $d < d_T$ compared to the other coded schemes. These results come from the flexibility of the LT code to adjust its rate to suit instantaneous channel conditions, and suggest that LT codes are beneficial in practical low-power WSNs with dynamic position sensor nodes.

Index Terms

Wireless sensor networks, energy efficiency, green modulation, LT codes.

^{††}The second author completed his Ph.D. in ECE at University of Toronto.

I. INTRODUCTION

Wireless Sensor Networks (WSNs) have been recognized as a new generation of ubiquitous computing systems to support a broad range of applications, including monitoring, health care and tracking environmental pollution levels. Minimizing the total energy consumption in both circuit components and RF signal transmission is a crucial challenge in designing a WSN. Central to this study is to find energy-efficient modulation and coding schemes in the physical layer of a WSN to prolong the sensor lifetime [2], [3]. For this purpose, energy-efficient modulation/coding schemes should be simple enough to be implemented by state-of-the-art low-power technology, but still robust enough to provide the desired service. Furthermore, since sensor nodes frequently switch from sleep mode to active mode, modulation and coding circuits should have fast start-up times [4] along with the capability of transmitting packets during a pre-assigned time slot before new sensed packets arrive. In addition, a WSN needs a powerful channel coding scheme which protects transmitted data against the unpredictable and harsh nature of channels. Finally, since coding increases the required transmitted bandwidth, when considered independently of modulation, the best tradeoff between energy-efficient modulation and coding for a given transmission bandwidth should be considered as well. We refer to these low-complexity and low-energy consumption approaches in WSNs providing proper link reliability without increasing a given transmission bandwidth as *Green Modulation/Coding* (GMC) schemes.

There have been several recent works on the energy efficiency of various modulation and channel coding schemes in WSNs (see e.g., [2], [5], [6]). Tang *et al.* [5] analyze the power efficiency of Pulse Position Modulation (PPM) and Frequency Shift Keying (FSK) in a WSN without considering the effect of channel coding. Under the assumption of the non-linear battery model, reference [5] shows that FSK is more power-efficient than PPM in sparse WSNs, while PPM may outperform FSK in dense WSNs. Reference [7] investigates the energy efficiency of BCH and convolutional codes with non-coherent FSK for the optimal packet length in a point-to-point WSN. It is shown in [7] that BCH codes can improve energy efficiency compared to the convolutional code for optimal fixed packet size. Reference [8] analyzes the effect of different linear block channel codes with FSK modulation on energy consumptions of a low-power wireless embedded network when the number of hops increases. Liang *et al.* [9] investigate the

energy efficiency of uncoded NC-MFSK modulation scheme in a multiple-access WSN over Rayleigh fading channels, where multiple senders transmit their data to a central node in a Frequency-Division Multiple Access (FDMA) fashion. Reference [10] presents the hardware implementation of the Forward Error Correction (FEC) encoder in IEEE 802.15.4 WSNs, which employs parallel just-in-time processing to achieve a low processing latency and energy consumption.

Most of the pioneering works on energy-efficient modulation/coding, including research in [5], [7], [8], [11], [12], has focused only on minimizing the energy consumption of transmitting one bit, ignoring the effect of bandwidth and transmission time duration. In a practical WSN however, it is shown that minimizing the total energy consumption depends strongly on the active mode duration and the channel bandwidth. References [1], [2] and [6] address this issue in a point-to-point WSN, where a sensor node transmits an equal amount of data per time unit to a designated sink node. In [2], the authors consider the optimal energy consumption per information bit as a function of modulation and coding parameters in a WSN over Additive White Gaussian Noise (AWGN) channels with path-loss. It is shown in [2] that uncoded MQAM is more energy-efficient than uncoded MFSK for short-range applications. For higher distance, however, using convolutional coded MFSK over AWGN is desirable. This line of work is further extended in [6] by evaluating the energy consumption per information bit of a WSN for Reed Solomon (RS) Codes and various modulation schemes over AWGN channels with path-loss. Also, the impact of different transmission distances on the energy consumption per information bit is investigated in [6]. In [2] and [6], the authors do not consider the effect of multi-path fading. Reference [1] addresses this problem in a similar WSN model as [2] and [6], and shows that among various sinusoidal carrier-based modulation schemes, Non-Coherent M-ary Frequency Shift Keying (NC-MFSK) with small order of constellation size M can be considered the most energy-efficient modulation in proactive WSNs over Rayleigh and Rician fading channels. However, no channel coding scheme was considered in [1].

More recently, the attention of researchers has been drawn to deploying rateless codes (e.g., Luby Transform (LT) code [13]) in WSNs due to the outstanding advantages of these codes in *erasure channels*. For instance in [14], the authors present a scheme for cooperative error control coding using rateless and Low-Density Generator-Matrix (LDGM) codes in a multiple relay WSN. However, investigating the

energy efficiency of rateless codes in WSNs with green modulations over realistic fading channel models has received little attention. To the best of our knowledge, there is no existing analysis on the energy efficiency of rateless coded modulation that considers the effect of channel bandwidth and active mode duration on the total energy consumption in a practical proactive WSN. This paper addresses this problem and presents the first in-depth analysis of the energy efficiency of LT codes with NC-MFSK (known as green modulation) as described in [1]. The present analysis is based on a realistic model in proactive WSNs operating in a Rayleigh flat-fading channel with path-loss. In addition, we obtain numerically the probability mass function of the LT code rate and the corresponding coding gain, and study their effects on the energy efficiency of the WSN. This study uses the classical BCH and convolutional codes (as reference codes), utilized in IEEE standards, for comparative evaluation. Experimental results show that the optimized LT coded NC-MFSK is the most energy-efficient scheme for distance d greater than the threshold level d_T . In addition, although uncoded NC-MFSK outperforms coded schemes for $d < d_T$, the energy gap between LT coded and uncoded NC-MFSK is negligible for $d < d_T$ compared to the other coded schemes. This result comes from the simplicity and flexibility of the LT codes, and suggests that LT codes are beneficial in practical low-power WSNs with dynamic position sensor nodes.

The rest of the paper is organized as follows. In Section II, the proactive system model over a realistic wireless channel model is described. The energy consumption of uncoded NC-MFSK modulation scheme is analyzed in Section III. Design of LT codes and the energy efficiency of the LT coded NC-MFSK are presented in Section IV. In addition, the energy efficiency of some classical channel codes are studied in this section. Section V provides some numerical evaluations using realistic models to confirm our analysis. Also, some design guidelines for using LT codes in practical WSN applications are presented. Finally in Section VI, an overview of the results and conclusions are presented.

For convenience, we provide a list of key mathematical symbols used in this paper in Table I.

II. SYSTEM MODEL AND ASSUMPTIONS

In this work, we consider a *proactive* wireless sensor system, in which a sensor node continuously samples the environment and transmits an equal amount of data per time unit to a designated sink node. Such a proactive sensor system is typical of many environmental applications such as sensing temperature,

TABLE I

LIST OF NOTATIONS

B	Channel bandwidth
d	Transmission distance
\mathcal{E}_t	Energy of uncoded transmitted signal
\mathcal{E}_N	Total energy consumption for uncoded case
h_i	Fading channel coefficient for symbol i
\mathcal{L}_d	Channel gain factor with distance d
M	Constellation size
N	Number of sensed message
n	Codeword block length
$\mathcal{O}(x)$	Output-node degree distribution
\mathcal{P}_c	Circuit power consumption
\mathcal{P}_t	Power of transmitted signal
P_b	Bit error rate
$P_R(\ell)$	pmf of LT code rate
R_c	Code rate
T_{ac}	Active mode duration
T_s	Symbol duration
η	Path-loss exponent
Ω	$\mathbb{E}[h_i ^2]$
γ_i	Instantaneous SNR
Υ_c	Coding gain

humidity, level of contamination, etc [15]. For this proactive system, the sensor and sink nodes synchronize with one another and operate in a real time-based process as depicted in Fig 1. During *active mode* duration T_{ac} , the analog signal sensed by the sensor is first digitized by an Analog-to-Digital Converter (ADC), and an N -bit message sequence $\mathcal{M}_N \triangleq (m_1, m_2, \dots, m_N)$ is generated, where N is assumed to be fixed, and $m_i \in \{0, 1\}$, $i = 1, 2, \dots, N$. The bit stream is then sent to the channel encoder. The encoding process begins by dividing the uncoded message \mathcal{M}_N into blocks of equal length denoted by $\mathcal{B}_j \triangleq (m_{(j-1)k+1}, \dots, m_{jk})$, $j = 1, \dots, \frac{N}{k}$, where k is the length of any particular \mathcal{B}_j , and N is assumed to be divisible by k . Each block \mathcal{B}_j is encoded by a pre-determined channel coding scheme to generate a

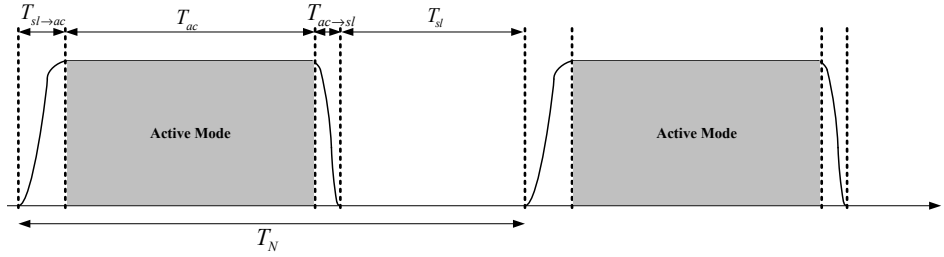


Fig. 1. A practical multi-mode operation in a proactive WSN.

coded bit stream $\mathcal{C}_j \triangleq (a_{(j-1)n+1}, \dots, a_{jn})$, $j = 1, \dots, \frac{N}{k}$, with block length n , where n is either a fixed value (e.g., for block and convolutional codes) or a random variable (e.g., for LT codes).

The coded stream is then modulated by an NC-MFSK scheme and transmitted to a designated sink node. Finally, the sensor node returns to *sleep mode*, and all the circuits of the transceiver are shutdown for sleep mode duration T_{sl} for energy saving. We denote T_{tr} as the *transient mode* duration consisting of the switching time from sleep mode to active mode (i.e., $T_{sl \rightarrow ac}$) plus the switching time from active mode to sleep mode (i.e., $T_{ac \rightarrow sl}$), where $T_{ac \rightarrow sl}$ is short enough compared to $T_{sl \rightarrow ac}$ to be negligible. Furthermore, when the sensor switches from sleep mode to active mode to send data, a significant amount of power is consumed for starting up the transmitter, while the power consumption during $T_{ac \rightarrow sl}$ is negligible. Under the above considerations, the sensor/sink nodes have to process one entire N -bit message \mathcal{M}_N during $0 \leq T_{ac} \leq T_N - T_{tr}$, before a new sensed packet arrives, where $T_N \triangleq T_{tr} + T_{ac} + T_{sl}$ is fixed, and $T_{tr} \approx T_{sl \rightarrow ac}$.

Since sensor nodes in a typical WSN are densely deployed, the distance between nodes is normally short. Thus, the circuit power consumption in a WSN is comparable to the output transmit power consumption. We denote the total circuit power consumption as $\mathcal{P}_c \triangleq \mathcal{P}_{ct} + \mathcal{P}_{cr}$, where \mathcal{P}_{ct} and \mathcal{P}_{cr} represent the circuit power consumptions for sensor and sink nodes, respectively. In addition, the power consumption of RF signal transmission in the sensor node is denoted by \mathcal{P}_t . Taking these into account, the total energy consumption during the active mode period, denoted by \mathcal{E}_{ac} , is given by $\mathcal{E}_{ac} = (\mathcal{P}_c + \mathcal{P}_t)T_{ac}$. Also, the energy consumption in the sleep mode period, denoted by \mathcal{E}_{sl} , is given by $\mathcal{E}_{sl} = \mathcal{P}_{sl}T_{sl}$, where \mathcal{P}_{sl} is the corresponding power consumption. It is worth mentioning that during the sleep mode interval, the *leakage current* coming from the CMOS circuits embedded in the sensor node is a dominant factor in \mathcal{P}_{sl} . Clearly,

higher sleep mode duration increases the energy consumption \mathcal{E}_{sl} due to increasing leakage current as well as T_{sl} . Present state-of-the art technology aims to keep a low sleep mode leakage current no larger than the battery leakage current, which results in \mathcal{P}_{sl} much smaller than the power consumption in active mode [16]. For this reason, we assume that $\mathcal{P}_{sl} \approx 0$. As a result, we have the following definition.

Definition 1 (Performance Metric): *The energy efficiency, referred to as the performance metric of the proposed WSN, can be measured by the total energy consumption in each period T_N corresponding to N -bit message \mathcal{M}_N as follows:*

$$\mathcal{E}_N = (\mathcal{P}_c + \mathcal{P}_t)T_{ac} + \mathcal{P}_{tr}T_{tr}, \quad (1)$$

where \mathcal{P}_{tr} is the circuit power consumption during the transient mode period.

We use (1) to investigate and compare the energy efficiency of uncoded and coded NC-MFSK for various channel coding schemes.

Channel Model: The choice of low transmission power in WSNs results in several consequences to the channel model. It is shown by Friis [17] that a low transmission power implies a small range. For short-range transmission scenarios, the root mean square (rms) delay spread is in the range of nanoseconds [18] which is small compared to symbol durations for modulated signals. For instance, the channel bandwidth and the corresponding symbol duration considered in the IEEE 802.15.4 standard are $B = 62.5$ KHz and $T_s = 16 \mu s$, respectively [19, p. 49], while the rms delay spread in indoor environments are in the range of 70-150 ns [20]. Thus, it is reasonable to expect a flat-fading channel model for WSNs. In addition, many transmission environments include significant obstacle and structural interference by obstacles (such as wall, doors, furniture, etc), which leads to reduced Line-Of-Sight (LOS) components. This behavior suggests a Rayleigh fading channel model. Under the above considerations, the channel model between the sensor and sink nodes is assumed to be Rayleigh flat-fading with path-loss, which is a feasible model in static WSNs [5], [11]. For this model, we assume that the channel is constant during the transmission of a codeword, but may vary from one codeword to another. We denote the fading channel coefficient corresponding to an arbitrary transmitted symbol i as h_i , where the amplitude $|h_i|$ is Rayleigh distributed with probability density function (pdf) given according to $f_{|h_i|}(r) = \frac{2r}{\Omega}e^{-\frac{r^2}{\Omega}}$, $r \geq 0$, where $\Omega \triangleq \mathbb{E}[|h_i|^2]$

(e.g., pp. 767-768 of [21]). This results in $|h_i|^2$ being *chi-square* distributed with 2 degrees of freedom, where $f_{|h_i|^2}(r) = \frac{1}{\Omega}e^{-\frac{r}{\Omega}}$, $r \geq 0$.

To model the path-loss of a link where the transmitter and receiver are separated by distance d , let denote \mathcal{P}_t and \mathcal{P}_r as the transmitted and the received signal powers, respectively. For a η^{th} -power path-loss channel, the channel gain factor is given by $\mathcal{L}_d \triangleq \frac{\mathcal{P}_t}{\mathcal{P}_r} = M_l d^\eta \mathcal{L}_1$, where M_l is the gain margin which accounts for the effects of hardware process variations, background noise and $\mathcal{L}_1 \triangleq \frac{(4\pi)^2}{\mathcal{G}_t \mathcal{G}_r \lambda^2}$ is the gain factor at $d = 1$ meter which is specified by the transmitter and receiver antenna gains \mathcal{G}_t and \mathcal{G}_r , and wavelength λ (e.g., [2], [11], Ch. 4 of [22] and [23]). As a result, when both fading and path-loss are considered, the instantaneous channel coefficient corresponding to an arbitrary symbol i becomes $G_i \triangleq \frac{h_i}{\sqrt{\mathcal{L}_d}}$. Denoting $x_i(t)$ as the RF transmitted signal with energy \mathcal{E}_t , the received signal at the sink node is given by $y_i(t) = G_i x_i(t) + n_i(t)$, where $n_i(t)$ is AWGN at the sink node with two-sided power spectral density given by $\frac{N_0}{2}$. Under the above considerations, the instantaneous Signal-to-Noise Ratio (SNR), denoted by γ_i , corresponding to an arbitrary symbol i can be computed as $\gamma_i = \frac{|G_i|^2 \mathcal{E}_t}{N_0}$. Under the assumption of a Rayleigh fading channel model, γ_i is chi-square distributed with 2 degrees of freedom and with pdf $f_\gamma(\gamma_i) = \frac{1}{\bar{\gamma}} e^{-\frac{\gamma_i}{\bar{\gamma}}}$, where $\bar{\gamma} \triangleq \mathbb{E}[|G_i|^2] \frac{\mathcal{E}_t}{N_0} = \frac{\Omega}{\mathcal{L}_d} \frac{\mathcal{E}_t}{N_0}$ denotes the average received SNR.

III. ENERGY CONSUMPTION OF UNCODED NC-MFSK MODULATION

We first consider uncoded MFSK modulation in the proposed proactive WSN, where M orthogonal carriers can be mapped into $b \triangleq \log_2 M$ bits. Denoting \mathcal{E}_t as the uncoded MFSK transmit energy per symbol with symbol duration T_s , the transmitted signal from the sensor node is given by $x_i(t) = \sqrt{\frac{2\mathcal{E}_t}{T_s}} \cos(2\pi(f_0 + i\Delta f)t)$, $i = 0, 1, \dots, M-1$, where f_0 is the first carrier frequency in the MFSK modulator and $\Delta f = \frac{1}{T_s}$ is the minimum carrier separation in the non-coherent case. Thus, the channel bandwidth is obtained as $B \approx M \times \Delta f$, which is assumed to be a fixed value. Since we have b bits during each symbol period T_s , we can write

$$T_{ac} = \frac{N}{b} T_s = \frac{MN}{B \log_2 M}. \quad (2)$$

Recalling that B and N are fixed, an increase M results in an increase in T_{ac} . However, as illustrated in Fig. 1, the maximum value for T_{ac} is bounded by $T_N - T_{tr}$. Thus, the maximum constellation size M ,

denoted by $M_{max} \triangleq 2^{b_{max}}$, for uncoded MFSK is calculated by $\frac{2^{b_{max}}}{b_{max}} = \frac{B}{N}(T_N - T_{tr})$. It is shown in [1] that the transmit energy consumption per each symbol for an uncoded NC-MFSK is obtained as

$$\mathcal{E}_t \triangleq \mathcal{P}_t T_s \approx \left[\left(1 - (1 - P_s)^{\frac{1}{M-1}} \right)^{-1} - 2 \right] \frac{\mathcal{L}_d N_0}{\Omega} \quad (3)$$

$$\stackrel{(a)}{\approx} \left[\left(1 - \left(1 - \frac{2(M-1)}{M} P_b \right)^{\frac{1}{M-1}} \right)^{-1} - 2 \right] \frac{\mathcal{L}_d N_0}{\Omega}, \quad (4)$$

where (a) comes from the fact that the relationship between the average Symbol Error Rate (SER) P_s and the average Bit Error Rate (BER) P_b of MFSK is given by $P_s = \frac{2(M-1)}{M} P_b$ [21, p. 262]. Using (2), the output energy consumption of transmitting N -bit during T_{ac} of an uncoded NC-MFSK is then computed as

$$\mathcal{P}_t T_{ac} = \frac{T_{ac}}{T_s} \mathcal{E}_t \approx \left[\left(1 - \left(1 - \frac{2(M-1)}{M} P_b \right)^{\frac{1}{M-1}} \right)^{-1} - 2 \right] \frac{\mathcal{L}_d N_0}{\Omega} \frac{N}{\log_2 M}. \quad (5)$$

For the sensor node with uncoded MFSK, we denote the power consumption of frequency synthesizer, filters and power amplifier as \mathcal{P}_{Sy} , \mathcal{P}_{Filt} and \mathcal{P}_{Amp} , respectively. In this case, the power consumption of the sensor circuitry with uncoded MFSK can be obtained as

$$\mathcal{P}_{ct} = \mathcal{P}_{Sy} + \mathcal{P}_{Filt} + \mathcal{P}_{Amp}, \quad (6)$$

where $\mathcal{P}_{Amp} = \alpha \mathcal{P}_t$, in which α is determined based on the type (or equivalently drain efficiency) of power amplifier. For instance, for a class B power amplifier, $\alpha = 0.33$ [2], [5]. It is shown in [1] that the power consumption of the sink circuitry with uncoded NC-MFSK scheme can be obtained as

$$\mathcal{P}_{cr} = \mathcal{P}_{LNA} + M \times (\mathcal{P}_{Filt} + \mathcal{P}_{ED}) + \mathcal{P}_{IFA} + \mathcal{P}_{ADC}, \quad (7)$$

where \mathcal{P}_{LNA} , \mathcal{P}_{Filt} , \mathcal{P}_{ED} , \mathcal{P}_{IFA} and \mathcal{P}_{ADC} denote the power consumption of Low-Noise Amplifier (LNA), filters, envelop detector, IF amplifier and ADC, respectively. In addition, it is shown that the power consumption during transition mode period T_{tr} is governed by the frequency synthesizer [4]. Thus, the energy consumption during T_{tr} is obtained as $\mathcal{P}_{tr} T_{tr} = 1.75 \mathcal{P}_{Sy} T_{tr}$ [18]. Substituting (2)-(7) in (1), the total energy consumption of an uncoded NC-MFSK scheme for transmitting N -bit information in each period T_N , under the constraint $M \leq M_{max}$ and for a given P_b is obtained as

$$\mathcal{E}_N = (1+\alpha) \left[\left(1 - \left(1 - \frac{2(M-1)}{M} P_b \right)^{\frac{1}{M-1}} \right)^{-1} - 2 \right] \frac{\mathcal{L}_d N_0}{\Omega} \frac{N}{\log_2 M} + (\mathcal{P}_c - \mathcal{P}_{Amp}) \frac{MN}{B \log_2 M} + 1.75 \mathcal{P}_{Sy} T_{tr}. \quad (8)$$

It is shown in [1] that the above uncoded NC-MFSK is more energy-efficient than other sinusoidal carrier-based modulation schemes, and is a good option for low-power and low data rate WSN applications. For energy optimal designs, however, the impact of channel coding on the energy efficiency of the proposed WSN must be considered as well. It is a well known fact that channel coding is a classical approach used to improve the link reliability along with the transmitter energy saving due to providing the coding gain [21]. However, the energy saving comes at the cost of extra energy spent in transmitting the redundant bits in codewords as well as the additional energy consumption in the process of encoding/decoding. For a specific transmission distance d , if these extra energy consumptions outweigh the transmit energy saving due to the channel coding, the coded system would not be energy-efficient compared with an uncoded system. In the subsequent sections, we will argue the above problem and determine at what distance use of specific channel coding becomes energy-efficient compared to uncoded systems. In particular, we will show in Section V that the LT coded NC-MFSK surpasses this distance constraint in the proposed WSN.

IV. ENERGY CONSUMPTION ANALYSIS OF LT CODED NC-MFSK

In this section, we present the first in-depth analysis on the energy efficiency of LT coded NC-MFSK for the proposed proactive WSN. To get more insight into how channel coding affects the circuit and RF signal energy consumptions in the system, we modify the energy concepts in Section III, in particular, the total energy consumption expression in (8) based on the coding gain and code rate. To address this problem and for the purpose of comparative evaluation, we first start with classical BCH and convolutional channel codes (referred to as fixed-rate codes), that are widely utilized in IEEE standards [24], [25]. We further present the first study on the tradeoff between LT code rate and coding gain required to achieve a certain BER, and the effect of this tradeoff on the total energy consumption of LT coded NC-MFSK for different transmission distances¹.

BCH Codes: In the BCH(n, k, t) code with up to t -error correction capability, each k -bit message $\mathcal{B}_j \in \mathcal{M}_N$ is encoded into $2^{nR_c^{BC}}$ valid codewords $\mathcal{C}_j \triangleq (a_{(j-1)n+1}, \dots, a_{jn})$, $j = 1, \dots, \frac{N}{k}$ with block length n , where $R_c^{BC} \triangleq \frac{k}{n}$ is the BCH code rate. For this code, $n = 2^m - 1$ bits, where $m \geq 3$, $t < 2^{m-1}$ and the number of parity-check bits is upper bounded by $n - k \leq mt$. It is worth mentioning that the number

¹In the sequel and for simplicity of notation, we use the superscripts ‘BC’, ‘CC’ and ‘LT’ for BCH, convolutional and LT codes, respectively.

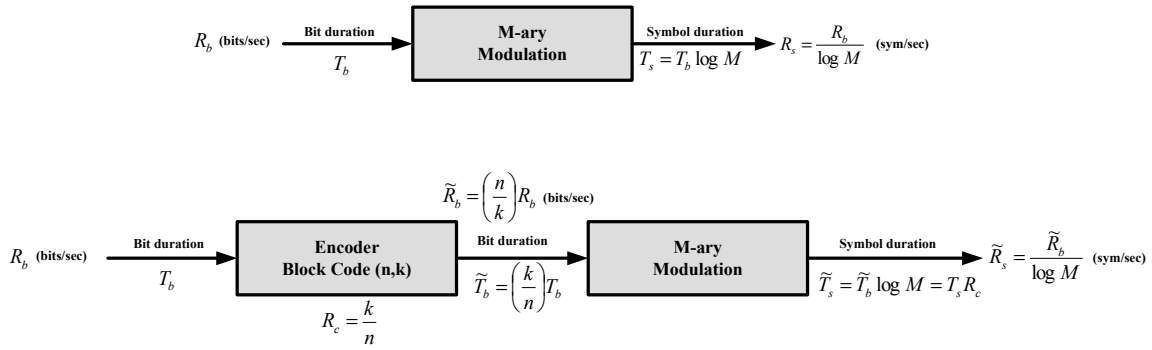


Fig. 2. A schematic diagram of the bandwidth expansion in an arbitrary block code (n, k) with M-ary modulation scheme.

of transmitted bits in each period T_N is increased from N -bit uncoded message to $\frac{N}{R_c^{BC}} = \frac{N}{k}n$ bits coded one. To compute the total energy consumption of coded scheme, we use the fact that channel coding can reduce the required average SNR value to achieve a given BER. Taking this into account, the proposed WSN with BCH codes benefits in transmission energy saving specified by $\mathcal{E}_t^{BC} = \frac{\mathcal{E}_t}{\Upsilon_c^{BC}}$, where $\Upsilon_c^{BC} \geq 1$ is the coding gain² of BCH coded NC-MFSK. Table II displays the coding gain of some BCH (n, k, t) codes with NC-MFSK scheme over a Rayleigh flat-fading channel for different values of M and given $P_b = (10^{-3}, 10^{-4})$. For these results, a hard-decision decoding algorithm is considered. It is seen from Table II that there is a tradeoff between coding gain and decoder complexity. In fact, achieving a higher coding gain for given M , requires a more complex decoding process, (i.e., higher t) with more circuit power consumption.

It should be noted that the cost of the energy savings of using BCH codes is the bandwidth expansion $\frac{B}{R_c^{BC}}$ as depicted in Fig. 2. In order to keep the bandwidth of the coded system the same as that of the uncoded case, we must keep the information transmission rate constant, i.e., the symbol duration T_s of uncoded and coded NC-MFSK would be the same. Thus, we can drop the superscript “BC” in T_s for the coded case. However, the active mode duration increases from $T_{ac} = \frac{N}{b}T_s$ in the uncoded system to

$$T_{ac}^{BC} = \frac{N}{bR_c^{BC}}T_s = \frac{T_{ac}}{R_c^{BC}} \quad (9)$$

for the BCH coded case. Thus, one would assume that the total time T_N increases to $\frac{T_N}{R_c^{BC}}$ for the coded scenario. It should be noted that the maximum constellation size M , denoted by $M_{max} \triangleq 2^{b_{max}}$, for the

²Denoting $\bar{\gamma} = \frac{\Omega}{\mathcal{L}_d} \frac{\mathcal{E}_t}{N_0}$ and $\bar{\gamma}^{BC} = \frac{\Omega}{\mathcal{L}_d} \frac{\mathcal{E}_t^{BC}}{N_0}$ as the average SNR of uncoded and BCH coded schemes, respectively, the BCH coding gain (expressed in dB) is defined as the difference between the values of $\bar{\gamma}$ and $\bar{\gamma}^{BC}$ required to achieve a certain BER, where $\mathcal{E}_t^{BC} = \frac{\mathcal{E}_t}{\Upsilon_c^{BC}}$.

TABLE II

CODING GAIN (dB) OF BCH(n, k, t) AND CONVOLUTIONAL CODED NC-MFSK OVER RAYLEIGH FLAT-FADING CHANNEL FOR

BER = ($10^{-3}, 10^{-4}$).

BCH Code	R_c^{BC}	M=2	M=4	M=8	M=16	M=32	M=64
BCH (7, 4, 1)	0.571	(2.5, 2.8)	(0.3, 0.4)	(0.1, 0.2)	(0.0, 0.0)	(0.0, 0.0)	(0.0, 0.0)
BCH (15, 11, 1)	0.733	(1.4, 1.6)	(0.2, 0.3)	(0.0, 0.0)	(0.0, 0.0)	(0.0, 0.0)	(0.0, 0.0)
BCH (15, 7, 2)	0.467	(2.4, 3.3)	(2.0, 2.3)	(0.8, 1.0)	(0.3, 0.4)	(0.0, 0.0)	(0.0, 0.0)
BCH (15, 5, 3)	0.333	(4.1, 4.6)	(2.7, 2.9)	(2.0, 2.1)	(1.5, 1.60)	(0.7, 0.8)	(0.2, 0.2)
BCH (31, 26, 1)	0.839	(1.2, 1.5)	(0.2, 0.2)	(0.0, 0.0)	(0.0, 0.0)	(0.0, 0.0)	(0.0, 0.0)
BCH (31, 21, 2)	0.677	(2.3, 2.9)	(1.7, 2.0)	(0.7, 0.8)	(0.2, 0.2)	(0.0, 0.0)	(0.0, 0.0)
BCH (31, 16, 3)	0.516	(2.9, 3.1)	(2.1, 2.2)	(1.5, 1.6)	(1.3, 1.4)	(0.6, 0.7)	(0.1, 0.1)
BCH (31, 11, 5)	0.355	(4.1, 4.4)	(3.5, 4.2)	(2.2, 2.3)	(2.0, 2.1)	(1.8, 2.0)	(1.1, 1.3)
BCH (31, 6, 7)	0.194	(5.4, 5.9)	(4.3, 4.8)	(3.5, 3.8)	(3.2, 3.3)	(2.7, 2.8)	(2.3, 2.4)
Convolutional Code	R_c^{CC}	M=2	M=4	M=8	M=16	M=32	M=64
trel(6, [53 75])	0.500	(3.8, 4.6)	(2.7, 3.1)	(2.1, 2.3)	(1.8, 2.0)	(1.4, 1.5)	(1.4, 1.4)
trel(7, [133 171])	0.500	(4.0, 4.7)	(3.0, 3.5)	(2.2, 2.4)	(1.8, 2.0)	(1.5, 1.6)	(1.4, 1.5)
trel(7, [133 165 171])	0.333	(5.7, 6.4)	(4.8, 5.1)	(3.7, 3.9)	(3.1, 3.3)	(2.7, 2.8)	(2.5, 2.6)
trel([4 3], [4 5 17; 7 4 2])	0.667	(2.2, 2.6)	(1.5, 1.7)	(0.9, 1.1)	(0.6, 0.6)	(0.5, 0.5)	(0.5, 0.5)
trel([5 4], [23 35 0; 0 5 13])	0.667	(2.9, 3.5)	(1.9, 2.4)	(1.4, 1.8)	(1.1, 1.2)	(0.8, 0.9)	(0.7, 0.8)

coded NC-MFSK is calculated by $\frac{2^{b_{max}}}{b_{max}} = \frac{BR_c^{BC}}{N} (T_N^{BC} - T_{tr})$, which is approximately the same as that of the uncoded case.

Now, we are ready to compute the total energy consumption in the case of BCH coded NC-MFSK. Since BCH codes are implemented using Linear-Feedback Shift Register (LFSR) circuits, the BCH encoder can be assumed to have negligible energy consumption. Thus, the energy cost of the sensor circuitry with BCH coded NC-MFSK scheme is approximately the same as that of uncoded one. Also, the energy consumption of an BCH decoder is negligible compared to the other circuit components in the sink node, as shown in Appendix I. Substituting (4) in $\mathcal{E}_t^{BC} = \frac{\mathcal{E}_t}{\Upsilon^{BC}}$, and using (6), (7) and (9), the total energy consumption of transmitting $\frac{N}{R_c^{BC}}$ bits in each period $\frac{T_N}{R_c^{BC}}$ for a BCH coded NC-MFSK scheme, and for a given P_b is

obtained as

$$\begin{aligned} \mathcal{E}_N^{BC} = (1 + \alpha) & \left[\left(1 - \left(1 - \frac{2(M-1)}{M} P_b \right)^{\frac{1}{M-1}} \right)^{-1} - 2 \right] \frac{\mathcal{L}_d N_0}{\Omega \Upsilon_c^{BC}} \frac{N}{R_c^{BC} \log_2 M} + \\ & (\mathcal{P}_c - \mathcal{P}_{Amp}) \frac{MN}{BR_c^{BC} \log_2 M} + 1.75 \mathcal{P}_{Sy} T_{tr}, \end{aligned} \quad (10)$$

under the constraint $M \leq M_{max}$.

Convolutional Codes: A convolutional code (n, k, L) is commonly specified by the number of input bits k , the number of output bits n , and the constraint length³ L . As with BCH codes, the rate of a convolutional code is given by the ratio $R_c^{CC} \triangleq \frac{k}{n}$. Since k and n are small integers (typically from 1 to 8) with $k < n$, the convolutional encoder is extremely simple to implement and can be assumed to have negligible energy consumption. With a similar argument as for BCH codes, the convolutional coded NC-MFSK provides an energy saving compared to the uncoded system, which is specified by $\mathcal{E}_t^{CC} = \frac{\mathcal{E}_t}{\Upsilon_c^{CC}}$. Table II gives the coding gain Υ_c^{CC} of some practical convolutional codes used in IEEE standards with an NC-MFSK modulation scheme, over a Rayleigh flat-fading channel for different constellation size M and given $P_b = (10^{-3}, 10^{-4})$. For these results, a hard-decision Viterbi decoding algorithm is considered. It is seen from Table II that for a given M , the convolutional codes with lower rates and higher constraint lengths achieve greater coding gains. Also, in contrast to [2], where the authors assume a fixed convolutional coding gain for every value of M , it is observed that the coding gain of convolutional coded NC-MFSK is a monotonically decreasing function of M .

It should be noted that the energy efficiency analysis presented for BCH codes, in particular deriving the total energy consumption \mathcal{E}_N^{CC} , is valid for convolution codes. Thus, by substituting (4) in $\mathcal{E}_t^{CC} = \frac{\mathcal{E}_t}{\Upsilon_c^{CC}}$, and using (6), (7) and $T_{ac}^{CC} = \frac{N}{bR_c^{CC}} T_s$, the total energy consumption of transmitting $\frac{N}{R_c^{CC}}$ bits in each period $\frac{T_N}{R_c^{CC}}$ for a convolutional coded NC-MFSK scheme, achieving a certain P_b , is obtained as

$$\begin{aligned} \mathcal{E}_N^{CC} = (1 + \alpha) & \left[\left(1 - \left(1 - \frac{2(M-1)}{M} P_b \right)^{\frac{1}{M-1}} \right)^{-1} - 2 \right] \frac{\mathcal{L}_d N_0}{\Omega \Upsilon_c^{CC}} \frac{N}{R_c^{CC} \log_2 M} + \\ & (\mathcal{P}_c - \mathcal{P}_{Amp}) \frac{MN}{BR_c^{CC} \log_2 M} + 1.75 \mathcal{P}_{Sy} T_{tr}. \end{aligned} \quad (11)$$

³The constraint length L represents the number of bits in the encoder memory that affect the generation of the n output bits.

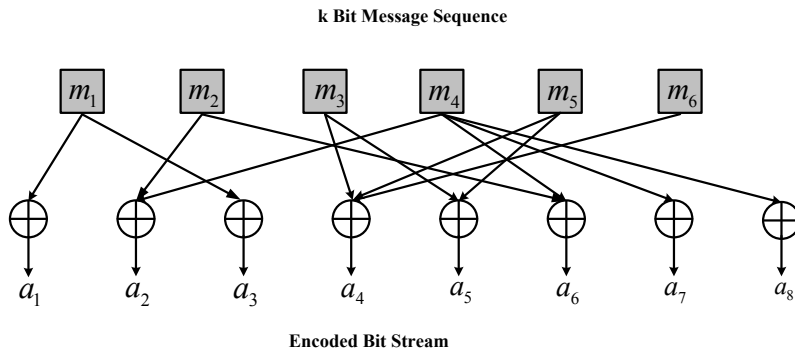


Fig. 3. Bipartite graph of an LT code with $k = 6$ and $n = 8$.

LT Codes: LT codes are the first class of Fountain codes (designed for erasure channels) that are near optimal erasure correcting codes [13]. The traditional schemes for data transmission across erasure channels use continuous two-way communication protocols, meaning that if the receiver can not decode the received packet correctly, asks the transmitter (via a feedback channel) to send the packet again. This process continues until all the packets have been decoded successfully. Fountain codes in general, and LT codes in particular, surpass the above feedback channel problem by adopting an essentially one-way communication approach.

LT codes are usually specified jointly by two parameters k (number of input bits) and $\mathcal{O}(x)$ (the output-node degree distribution). The encoding process begins by dividing the original message \mathcal{M}_N into blocks of equal length. Without loss of generality and for ease of our analysis, we use index $j = 1$, meaning a single k -bit message $\mathcal{B}_1 \triangleq (m_1, m_2, \dots, m_k) \in \mathcal{M}_N$ is encoded to codeword $\mathcal{C}_1 \triangleq (a_1, a_2, \dots, a_n)$. Each single coded bit a_i is generated based on the encoding protocol proposed in [13]: *i*) randomly choose a degree $1 \leq \mathcal{D} \leq k$ from a priori known degree distribution $\mathcal{O}(x)$, *ii*) using a uniform distribution, randomly choose \mathcal{D} distinct input bits, and calculate the encoded bit a_i as the XOR-sum of these \mathcal{D} bits. The above encoding process defines a sparse⁴ bipartite graph connecting encoded (or equivalently output) nodes to input nodes (see, e.g., Fig. 3). It is seen that the LT encoding process is extremely simple and has very low energy consumption. Unlike classical linear block and convolutional codes, in which the codeword block length is fixed, for the above LT code, n is a variable parameter, resulting in a random variable LT code rate $R_c^{LT} \triangleq \frac{k}{n}$. More precisely, $a_n \in \mathcal{C}_1$ is the last bit generated at the output

⁴If the mean degree \mathcal{D} is significantly smaller than k , then the graph is sparse.

of LT encoder before receiving the acknowledgement signal from the sink node indicating termination of a successful decoding process. This inherent property of LT codes means they can vary their codeword block lengths to adapt to any wireless channel condition.

We now turn our attention to the LT code design in the proposed WSN. As seen in the above encoding process, the output-node degree distribution is the most influential factor in the LT code design. On the one hand, we need high degree \mathcal{D} in order to ensure that there are no unconnected input nodes in the graph. On the other hand, we need low degree \mathcal{D} in order to keep the number of XOR-sum modules for decoding small. The latter characteristic means the WSN has less complexity and lower power consumption. To describe the output-node degree distribution used in this work, let $\mu_i, i = 1, \dots, k$, denote the probability that an output node has degree i . Following the notation of [26], the output-node degree distribution of an LT code has the polynomial form $\mathcal{O}(x) \triangleq \sum_{i=1}^k \mu_i x^i$ with the property that $\mathcal{O}(1) = \sum_{i=1}^k \mu_i = 1$. Typically, optimizing the output-node degree distribution for a specific wireless channel model is a crucial task in designing LT codes. The original output-node degree distribution for LT codes, namely the Robust Soliton distribution [13], intended for erasure channels, is not optimal for an error-channel and has poor error correcting capability. In fact, for wireless fading channels, it is still an open problem, what the “optimal” $\mathcal{O}(x)$ is. In this work, we use the following output-node degree distribution which was optimized for a BSC using a hard-decision decoder [27]:

$$\begin{aligned} \mathcal{O}(x) = & 0.00466x + 0.55545x^2 + 0.09743x^3 + 0.17506x^5 + 0.03774x^8 + 0.08202x^{14} + \\ & 0.01775x^{33} + 0.02989x^{100}. \end{aligned} \quad (12)$$

The LT decoder at the sink node can recover the original k -bit message \mathcal{B}_1 with high probability after receiving any $(1 + \epsilon)k$ bits in its buffer, where ϵ depends upon the LT code design [26]. For this recovery process, the LT decoder needs to correctly reconstruct the bipartite graph of an LT code. Clearly, this requires perfect synchronization between encoder and decoder, i.e., the LT decoder would need to know exactly the randomly generated degree \mathcal{D} for encoding original \mathcal{D} bits. One practical approach suitable for the proposed WSN model is that the LT encoder and decoder use identical pseudo-random generators with a common seed value which may reduce the complexity further. In this work, we assume that the sink node recovers k -bit message \mathcal{B}_1 using a simple hard-decision “*ternary message passing*” decoder in

a nearly identical manner to the “*Algorithm E*” decoder in [28] for Low-Density Parity-Check (LDPC) codes⁵. The main reason for using the ternary decoder here is to make a fair comparison to the BCH and convolutional codes, since those codes involved a hard-decision prior to decoding. Also, the degree distribution $\mathcal{O}(x)$ in (12) was optimized for a ternary decoder in a BSC and we are aware of no better $\mathcal{O}(x)$ for the ternary decoder in Rayleigh fading channels.

To analyze the total energy consumption of transmitting $\frac{N}{R_c^{LT}}$ bits during active mode period for LT coded NC-MFSK scheme, one would compute the LT code rate and the corresponding LT coding gain. Let us begin with the case of asymptotic LT code rate, where the number of input bits k goes to infinity. It is shown that the LT code rate is obtained asymptotically as a fixed value of $R_c^{LT} \approx \frac{\mathcal{O}_{ave}}{\mathcal{I}_{ave}}$ for large values of k , where \mathcal{O}_{ave} and \mathcal{I}_{ave} represent the average degree of the output and the input nodes in the bipartite graph, respectively (see Appendix II for the proof). When using finite- k LT codes in a fading channel, the instantaneous SNR changes from one codeword to the next. Consequently, the rate of the LT code for any block can be chosen to achieve the desired performance for that block (i.e., we can collect a sufficient number of bits to achieve a desired coded BER). This means that for any given average SNR, the LT code rate is described by either a probability mass function (pmf) or a probability density function (pdf) denoted by $P_R(\ell)$. Because it is difficult to get a closed-form expression of $P_R(\ell)$, we use a discretized numerical method to calculate the pmf $P_R(\ell) \triangleq \Pr\{R_c^{LT} = \ell\}$, $0 \leq \ell \leq 1$, for different values of M . Table III presents the pmfs of LT code rate for $M = 2$ and various average SNR over a Rayleigh fading channel model. To gain more insight into these results, we plot the pmfs of the LT code rate in Fig. 4 for the case of $M = 2$. It is observed that for lower average SNRs the pmfs are larger in the lower rate regimes (i.e., the pmfs spend more time in the low rate region). Also, all pmfs exhibit quite a spike for the highest rate, which makes sense since once the instantaneous SNR hits a certain critical value, the codes will always decode with a high rate. Also, Fig. 5 illustrates the pmf of LT code rates for various constellation size M and for average SNR equal to 16 dB. It can be seen that as M increases, the rate of the LT code tends to have a pmf with larger values in the lower rate regions.

⁵Description of the *ternary message passing* decoding is out of scope of this work, and the reader is referred to Chapter 4 in [27] for more details.

TABLE III

PROBABILITY MASS FUNCTION OF LT CODE RATE OVER RAYLEIGH FADING CHANNEL FOR VARIOUS AVERAGE SNR AND $M = 2$.

Code Rate	pmf (6 dB)	pmf (8 dB)	pmf (10 dB)	pmf (12 dB)	pmf (14 dB)	pmf (16 dB)	pmf (18 dB)	pmf (20 dB)	pmf (22 dB)	pmf (24 dB)	pmf (26 dB)
0.95	0.0101	0.0521	0.1380	0.3067	0.4742	0.6244	0.7429	0.8290	0.8884	0.9281	0.9540
0.90	0.0180	0.0514	0.0975	0.0978	0.0906	0.0728	0.0536	0.0372	0.0249	0.0164	0.0106
0.85	0.0222	0.0472	0.0841	0.0656	0.0563	0.0431	0.0307	0.0209	0.0138	0.0090	0.0058
0.80	0.0310	0.0540	0.0718	0.0613	0.0499	0.0370	0.0239	0.0174	0.0114	0.0070	0.0047
0.75	0.0442	0.0649	0.0608	0.0617	0.0382	0.0348	0.0189	0.0159	0.0104	0.0054	0.0043
0.70	0.0438	0.0563	0.0506	0.0466	0.0302	0.0248	0.0148	0.0111	0.0072	0.0043	0.0029
0.65	0.0375	0.0439	0.0409	0.0331	0.0244	0.0169	0.0114	0.0075	0.0048	0.0031	0.0020
0.60	0.0370	0.0405	0.0362	0.0285	0.0206	0.0142	0.0095	0.0062	0.0040	0.0026	0.0016
0.55	0.0355	0.0367	0.0317	0.0243	0.0174	0.0119	0.0079	0.0051	0.0033	0.0021	0.0013
0.50	0.0373	0.0369	0.0309	0.0233	0.0164	0.0111	0.0073	0.0048	0.0030	0.0019	0.0012
0.45	0.0345	0.0327	0.0286	0.0197	0.0158	0.0093	0.0065	0.0039	0.0025	0.0016	0.0010
0.40	0.0397	0.0362	0.0278	0.0210	0.0145	0.0097	0.0061	0.0041	0.0026	0.0016	0.0010
0.35	0.0395	0.0346	0.0269	0.0193	0.0132	0.0088	0.0057	0.0037	0.0023	0.0015	0.0009
0.30	0.0421	0.0356	0.0270	0.0192	0.0130	0.0086	0.0056	0.0036	0.0023	0.0015	0.0009
0.25	0.0440	0.0360	0.0278	0.0187	0.0126	0.0083	0.0054	0.0034	0.0022	0.0014	0.0009
0.20	0.0496	0.0393	0.0286	0.0197	0.0132	0.0086	0.0056	0.0035	0.0023	0.0014	0.0009
0.15	0.0541	0.0414	0.0295	0.0201	0.0133	0.0087	0.0056	0.0035	0.0023	0.0014	0.0009
0.10	0.0658	0.0486	0.0338	0.0227	0.0149	0.0097	0.0062	0.0039	0.0025	0.0016	0.0010
0.00	0.3138	0.2115	0.1392	0.0903	0.0579	0.0369	0.0235	0.0149	0.0094	0.0059	0.0038

Table IV illustrates the average LT code rates and the corresponding coding gains of LT coded NC-MFSK using $\mathcal{O}(x)$ in (12), for $M = 2, 4, 8, 16$ and given $P_b = 10^{-3}$. The average rate for a certain average SNR is obtained by integrating the pmf over the rates from 0 to 1. It is observed that the LT code is able to provide a huge coding gain Υ_c^{LT} given $P_b = 10^{-3}$, but this gain comes at the expense of a very low average code rate, which means many additional code bits need to be sent. This results in higher energy consumption per information bit. An interesting point extracted from Table IV is the flexibility of the LT code to adjust its rate (and its corresponding coding gain) to suit instantaneous channel conditions in WSNs. For instance in the case of favorable channel conditions, the LT coded NC-MFSK is able to

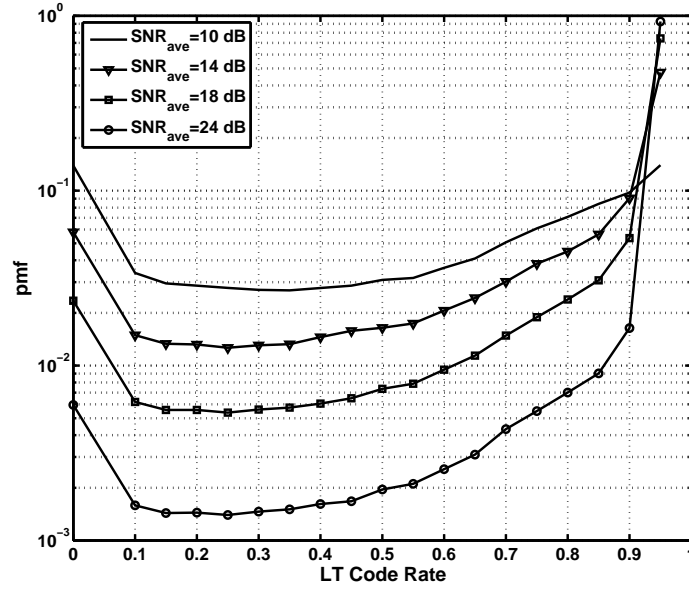


Fig. 4. The pmf of LT code rate for various average SNR and $M=2$.

achieve $R_c^{LT} \approx 1$ with $\Upsilon_c^{LT} \approx 0$ dB, which is similar to the case of uncoded NC-MFSK, i.e., $n = k$. In addition, by comparing the results in Table IV with those in Table II for BCH and convolutional codes, one observes that LT codes outperform the other coding schemes in energy saving at comparable rates. The effect of LT code rate flexibility on the total energy consumption is also observed in the simulation results in the subsequent section.

Unlike BCH and convolution codes in which the active mode duration of coded NC-MFSK is fixed, for the LT coded NC-MFSK, we have non-fixed values for $T_{ac}^{LT} = \frac{N}{bR_c^{LT}} T_s$. With a similar argument as for BCH and convolutional codes, the total energy consumption of transmitting $\frac{N}{R_c^{LT}}$ bits for a given P_b is obtained as a function of the random variable R_c^{LT} as follows:

$$\mathcal{E}_N^{LT} = (1 + \alpha) \left[\left(1 - \left(1 - \frac{2(M-1)}{M} P_b \right)^{\frac{1}{M-1}} \right)^{-1} - 2 \right] \frac{\mathcal{L}_d N_0}{\Omega \Upsilon_c^{LT}} \frac{N}{R_c^{LT} \log_2 M} + (\mathcal{P}_c - \mathcal{P}_{Amp}) \frac{MN}{BR_c^{LT} \log_2 M} + 1.75 \mathcal{P}_{Sy} T_{tr}, \quad (13)$$

where the goal is to minimize the average \mathcal{E}_N^{LT} over R_c^{LT} .

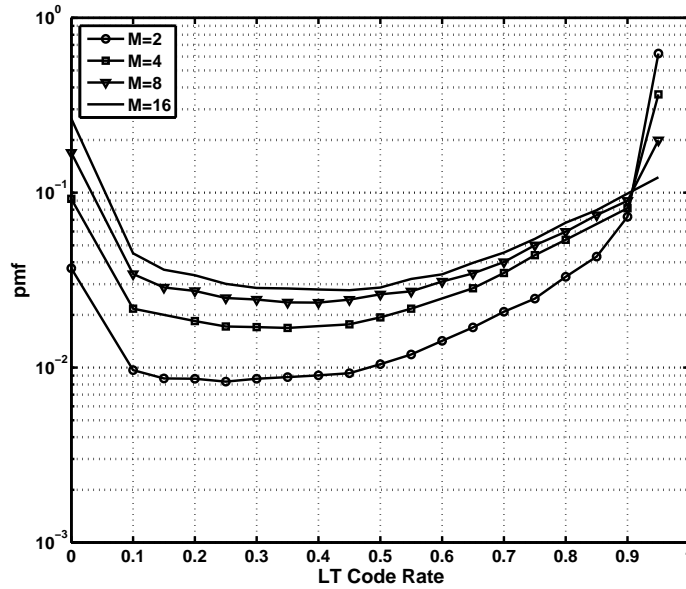


Fig. 5. The pmf of LT code rate for various constellation size M and average SNR=16 dB.

V. NUMERICAL RESULTS

In this section, we present some numerical evaluations using realistic parameters from the IEEE 802.15.4 standard and state-of-the-art technology to confirm the energy efficiency analysis of uncoded and coded NC-MFSK modulation schemes discussed in Sections III and IV. We assume that the NC-MFSK modulation scheme operates in the $f_0 = 2.4$ GHz Industrial Scientist and Medical (ISM) unlicensed band utilized in IEEE 802.15.4 for WSNs [19]. According to the FCC 15.247 RSS-210 standard for United States/Canada, the maximum allowed antenna gain is 6 dBi [29]. In this work, we assume that $\mathcal{G}_t = \mathcal{G}_r = 5$ dBi. Thus for $f_0 = 2.4$ GHz, \mathcal{L}_1 (dB) $\triangleq 10 \log_{10} \left(\frac{(4\pi)^2}{\mathcal{G}_t \mathcal{G}_r \lambda^2} \right) \approx 30$ dB, where $\lambda \triangleq \frac{3 \times 10^8}{f_0} = 0.125$ meters. We assume that in each period T_N , the sensed data frame size $N = 1024$ bytes (or equivalently $N = 8192$ bits) is generated, where T_N is assumed to be 1.4 seconds. The channel bandwidth is assumed to be $B = 62.5$ KHz, according to IEEE 802.15.4 [19, p. 49]. From $\frac{2^{b_{max}}}{b_{max}} = \frac{B}{N}(T_N - T_{tr})$, we find that $M_{max} \approx 64$ (or equivalently $b_{max} \approx 6$) for NC-MFSK. The power consumption of the LNA and IF amplifier are considered 9 mw [30] and 3 mw [2], [5], respectively. The power consumption of the frequency synthesizer is supposed to be 10 mw [4]. Table V summarizes the system parameters for simulation. The results in Tables II-IV are also used to compare the energy efficiency of uncoded and coded NC-MFSK schemes.

TABLE IV

AVERAGE LT CODE RATE AND CODING GAIN OF LT CODED NC-MFSK OVER RAYLEIGH FLAT-FADING MODEL FOR $P_b = 10^{-3}$ AND

M=2,4,8,16.

	M=2			M=4		M=8		M=16	
Average SNR (dB)	Average Code Rate	Coding Gain (dB)	Average SNR (dB)	Average Code Rate	Coding Gain (dB)	Average Code Rate	Coding Gain (dB)	Average Code Rate	Coding Gain (dB)
5	0.2560	25	0	0.0028	33.87	0.0012	36.46	0.0012	38.48
6	0.3174	24	2	0.0140	31.87	0.0024	34.46	0.0012	36.48
7	0.3819	23	4	0.0460	29.87	0.0095	32.46	0.0021	34.48
8	0.4475	22	6	0.1100	27.87	0.0330	30.46	0.0086	32.48
9	0.5120	21	8	0.2100	25.87	0.0870	28.46	0.0320	30.48
10	0.5738	20	10	0.3300	23.87	0.1800	26.46	0.0870	28.48
11	0.6315	19	12	0.4600	21.87	0.3000	24.46	0.1800	26.48
12	0.6840	18	14	0.5900	19.87	0.4400	22.46	0.3100	24.48
13	0.7307	17	16	0.7000	17.87	0.5700	20.46	0.4500	22.48
14	0.7716	16	18	0.7800	15.87	0.6800	18.46	0.5800	20.48
15	0.8067	15	20	0.8500	13.87	0.7700	16.46	0.6900	18.48
16	0.8365	14	22	0.8900	11.87	0.8400	14.46	0.7800	16.48
17	0.8614	13	24	0.9200	9.87	0.8800	12.46	0.8400	14.48
18	0.8821	12	26	0.9400	7.87	0.9100	10.46	0.8800	12.48
19	0.8991	11	28	0.9500	5.87	0.9300	8.46	0.9200	10.48
20	0.9130	10	30	0.9600	3.87	0.9500	6.46	0.9400	8.48
22	0.9333	8	32	0.9600	1.87	0.9500	4.46	0.9500	6.48
24	0.9466	6	34	0.9600	-0.13	0.9600	2.46	0.9500	4.48
26	0.9551	4	36	0.9700	-2.13	0.9600	0.46	0.9600	2.48
28	0.9606	2	38	0.9700	-4.13	0.9700	-1.54	0.9600	0.48
30	0.9640	0	40	0.9700	-6.13	0.9700	-3.54	0.9700	-1.52

TABLE V

SYSTEM EVALUATION PARAMETERS

$B = 62.5$ KHz	$N_0 = -180$ dB	$\mathcal{P}_{ADC} = 7$ mw
$M_l = 40$ dB	$\mathcal{P}_{Sy} = 10$ mw	$\mathcal{P}_{LNA} = 9$ mw
$\mathcal{L}_1 = 30$ dB	$\mathcal{P}_{Filt} = 2.5$ mw	$\mathcal{P}_{ED} = 3$ mw
$\eta = 3.5$	$\mathcal{P}_{Filt} = 2.5$ mw	$\mathcal{P}_{IFA} = 3$ mw
$\Omega = 1$	$T_N = 1.4$ sec	$T_{tr} = 5$ μ s

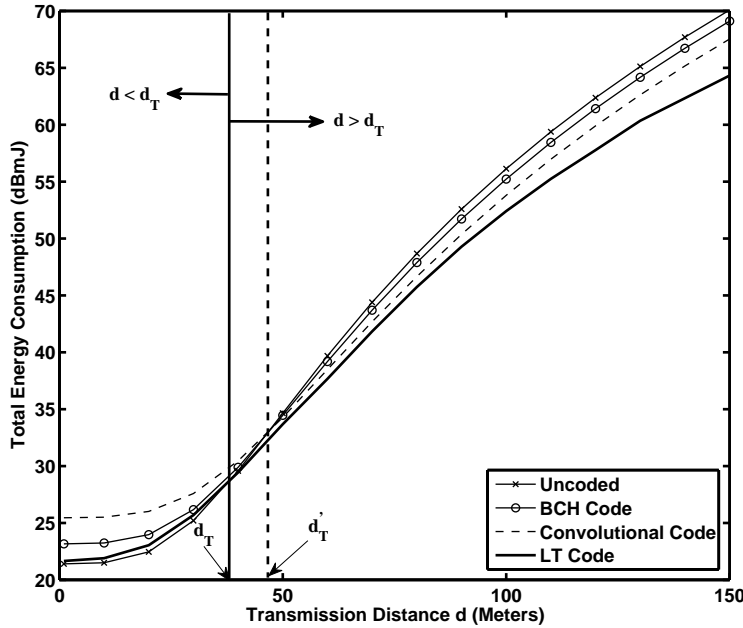


Fig. 6. Total energy consumption of optimized coded and uncoded NC-MFSK versus d for $P_b = 10^{-3}$.

Fig. 6 shows the total energy consumption versus distance d for the optimized BCH, convolutional and LT coded NC-MFSK schemes, compared to the optimized uncoded NC-MFSK for $P_b = 10^{-3}$. The optimization is done over M and the parameters of coding scheme. Simulation results show that for d less than the threshold level $d_T \approx 40$ m, the total energy consumption of optimized uncoded NC-MFSK is less than that of the coded NC-MFSK schemes. However, the energy gap between LT coded and uncoded NC-MFSK is negligible compared to the other coded schemes as expected. For $d > d_T$, the LT coded NC-MFSK scheme is more energy-efficient than uncoded and other coded NC-MFSK schemes. Also, it is observed that the energy gap between LT and convolutional coded NC-MFSK increases when the distance d grows. This result comes from the high coding gain capability of LT codes which confirms our analysis in Section IV. The threshold level d_T (for LT code) or d'_T (for BCH and convolutional codes) are obtained when the total energy consumptions of coded and uncoded systems become equal. For instance, using $\mathcal{L}_d = M_I d^\eta \mathcal{L}_1$, and the equality between (8) and (11) for uncoded and convolutional coded NC-MFSK,

we have

$$d'_T = \left[\frac{M\Omega(\mathcal{P}_c - \mathcal{P}_{Amp})}{(1 + \alpha) \left[\left(1 - \left(1 - \frac{2(M-1)}{M} P_b \right)^{\frac{1}{M-1}} \right)^{-1} - 2 \right]} \frac{1}{\mathcal{L}_1 M_l} \frac{\Upsilon_c^{CC}(1 - R_c^{CC})}{\Upsilon_c^{CC} R_c^{CC} - 1} \right]^{\frac{1}{\eta}}. \quad (14)$$

It should be noted that the above threshold level imposes a constraint on the design of the physical layer of some wireless sensor networking applications, in particular dynamic WSNs. To obtain more insight into this issue, let assume that the location of the sensor node is changed every $T_d \gg T_c$ time unit, where T_c is the channel coherence time. For the moment, let us assume that the sensor node aims to choose either a *fixed-rate coded* or an uncoded NC-MFSK based on the distance between sensor and sink nodes. According to the results in Fig. 6, it is revealed that using fixed-rate channel coding is not energy efficient for short distance transmission (i.e., $d < d'_T$), while for $d > d'_T$, convolutional coded NC-MFSK is more energy-efficient than other schemes. For this configuration, the sensor node must have the capability of an adaptive coding scheme for each distance d . However, as discussed previously, the LT codes can adjust their rates for each channel condition and have (with a good approximation) minimum energy consumption for every distance d . This indicates that LT codes can surpass the above distance constraint for WSN applications with dynamic position sensor nodes over Rayleigh fading channels. This characteristic of LT codes results in reducing the complexity of the network design as well. Of interest is the strong benefits of using LT coded NC-MFSK compared with the coded modulation schemes in [2], [6]. In contrast to classical fixed-rate codes used in [2], [6], the LT codes can vary their block lengths to adapt to any channel condition in each distance d . Unlike [2] and [6], where the authors consider fixed-rate codes over an AWGN channel model, we considered a Rayleigh fading channel which is a general model in practical WSNs. The simplicity and flexibility advantages of LT codes with an NC-MFSK scheme make them the preferable choice for wireless sensor networks, in particular for WSNs with dynamic position sensor nodes.

VI. CONCLUSION

In this paper, we analyzed the energy efficiency of LT coded NC-MFSK in a proactive WSN over Rayleigh fading channels with path-loss. It was shown that the energy efficiency of LT codes is similar to that of uncoded NC-MFSK scheme for $d < d_T$, while for $d > d_T$, LT coded NC-MFSK outperforms other uncoded and coded schemes, from the energy efficiency point of view. This result follows from the flexibility of the LT code to adjust its rate and the corresponding LT coding gain to suit instantaneous channel conditions for any transmission distance d . This rate flexibility offers strong benefits in using LT codes in practical WSNs with dynamic distance and position sensors. In such systems and for every value of distance d , LT codes can adjust their rates to achieve a certain BER with low energy consumption. The importance of our scheme is that it avoids some of the problems inherent in adaptive coding or Incremental Redundancy (IR) systems (channel feedback, large buffers, or multiple decodings), as well as the coding design challenge for fixed-rate codes used in WSNs with dynamic position sensor nodes. The simplicity and flexibility advantages of LT codes make the LT code with NC-MFSK modulation can be considered as a *Green Modulation/Coding* (GMC) scheme in dynamic WSNs.

APPENDIX I

ENERGY CONSUMPTION OF BCH DECODER

For the sink circuitry, we have an extra energy cost due to the decoding process in a coded NC-MFSK scheme. It is shown in [18, p. 160] that the energy consumption of an BCH(n, k, t) decoder per codeword, denoted by $\tilde{\mathcal{E}}_{Dec}^{BC}$, is computed as $\tilde{\mathcal{E}}_{Dec}^{BC} = (2nt + 2t^2)(\mathcal{E}_{add} + \mathcal{E}_{mult})$, where \mathcal{E}_{add} and \mathcal{E}_{mult} represent the energy consumptions of adder and multiplier in unit of W/MHz, respectively. For instance, the energy consumption of 0.5 μ W/MHz indicates that the consumed energy per clock cycle is 0.5 pJ. Thus, if for decoding of each bit we consider 20 clock cycles, the energy consumption is 10 pJ/bit. For this case, the total energy consumption a BCH(n, k, t) decoder to recover N -bit message \mathcal{M}_N is obtained as $\mathcal{E}_{Dec}^{BC} = \frac{N}{k}\tilde{\mathcal{E}}_{Dec}^{BC} = \frac{N}{k}(2nt + 2t^2)(\mathcal{E}_{add} + \mathcal{E}_{mult})$. It is shown in [31] that the energy consumption per addition or multiplication operation is on the order of pJ per bit. According to the values of n and t in Table II, one can with a good approximation assume that the energy consumption of an BCH decoder is

negligible compared to the other circuit components in the sink node.

APPENDIX II

ASYMPTOTIC LT CODE RATE

The proof of the remark is straightforward using the notation of [32] and the bipartite graph concepts in graph theory. Obviously, the output-node degree distribution $\mathcal{O}(x)$ induces a distribution on the input nodes in the bipartite graph. Thus, in the asymptotic case of $k \rightarrow \infty$, we have the input-node degree distribution defined as $\mathcal{I}(x) \triangleq \sum_{i=1}^{\infty} \nu_i x^i$, where ν_i denotes the probability that an input node has a degree i . In this case, the average degree of the input and output nodes are computed as $\left. \frac{d\mathcal{I}(x)}{dx} \right|_{x=1} \triangleq \mathcal{I}_{ave}$ and $\left. \frac{d\mathcal{O}(x)}{dx} \right|_{x=1} \triangleq \mathcal{O}_{ave}$, respectively. Thus, the number of edges exiting the input nodes of the bipartite graph, in the asymptotic case of $k \rightarrow \infty$, is $k\mathcal{I}_{ave}$, which must be equal to $n\mathcal{O}_{ave}$, the number of edges entering the output nodes in the graph. As a results, the asymptotic LT code rate is obtained as $R_c^{LT} = \frac{k}{n} \approx \frac{\mathcal{O}_{ave}}{\mathcal{I}_{ave}}$, which is a deterministic value for given $\mathcal{O}(x)$ and $\mathcal{I}(x)$.

REFERENCES

- [1] J. Abouei, K. N. Plataniotis, and S. Pasupathy, "Green modulation in proactive wireless sensor networks," *Submitted to IEEE Transactions on Wireless Communications*, Sept. 2009.
- [2] S. Cui, A. J. Goldsmith, and A. Bahai, "Energy-constrained modulation optimization," *IEEE Trans. on Wireless Commun.*, vol. 4, no. 5, pp. 2349–2360, Sept. 2005.
- [3] S. Howard, K. Iniewski, and C. Schlegel, "Error control coding in low-power wireless sensor networks: when is ECC energy-efficient?," *EURASIP Journal of Wireless Communications and Networking*, , no. 2, April 2006.
- [4] A. Y. Wang, S.-H. Cho, C. G. Sodini, and A. P. Chandrakasan, "Energy efficient modulation and MAC for asymmetric RF microsensor systems," in *Proc. of International Symposium on Low Power Electronics and Design (ISLPED'01)*. Huntington Beach, Calif, USA, Aug. 2001, pp. 106–111.
- [5] Q. Tang, L. Yang, G. B. Giannakis, and T. Qin, "Battery power efficiency of PPM and FSK in wireless sensor networks," *IEEE Trans. on Wireless Commun.*, vol. 6, no. 4, pp. 1308–1319, April 2007.
- [6] S. Chouhan, R. Bose, and M. Balakrishnan, "Integrated energy analysis of error correcting codes and modulation for energy efficient wireless sensor nodes," *IEEE Trans. on Wireless Commun.*, vol. 8, no. 10, pp. 5348–5355, Oct. 2009.
- [7] Y. Sankarasubramaniam, I. F. Akyildiz, and S. W. McLaughlin, "Energy efficiency based packet size optimization in wireless sensor networks," in *Proc. of IEEE International Workshop on Sensor Network Protocols and Applications*, 2003.
- [8] H. Karvonon, Z. Shelby, and C. Pomalaza-Raez, "Coding for energy efficient wireless embedded networks," in *Proc. of IEEE International Workshop on Wireless Ad-Hoc Networks*, June 2004, pp. 300–304.

- [9] X. Liang, W. Li, and T. A. Gulliver, "Energy efficient modulation design for wireless sensor networks," in *Proc. IEEE Pacific Rim Conf. on Commun., Computers and Signal Processing (PACRIM'07)*, Aug. 2007, pp. 98–101.
- [10] L. Li, R. G. Maunder, B. M. Al-Hashimi, and L. Hanzo, "An energy-efficient error correction scheme for IEEE 802.15.4 wireless sensor networks," *Submitted to IEEE Transactions on Circuits and Systems II*, 2009.
- [11] F. Qu, D. Duan, L. Yang, and A. Swami, "Signaling with imperfect channel state information: A battery power efficiency comparison," *IEEE Trans. on Signal Processing*, vol. 56, no. 9, pp. 4486–4495, Sep. 2008.
- [12] B. Shen and A. Abedi, "Error correction in heterogeneous wireless sensor networks," in *Proc. of 24th IEEE Biennial Symposium on Communication*. Kingston, Canada, June 2008.
- [13] M. Luby, "LT codes," in *Proc. of the 43rd Annual IEEE Symposium on Foundations of Computer Science (FOCS)*, 2002, pp. 271–280.
- [14] A. W. Eckford, J. P. K. Chu, and R. S. Adve, "Low-complexity cooperative coding for sensor networks using rateless and LDGM codes," in *Proc. of IEEE International Conference on Communications (ICC'06)*. Istanbul, Turkey, June 2006, pp. 1537–1542.
- [15] C. M. Cordeiro and D. P. Agrawal, *Ad Hoc and Sensor Networks: Theory and Applications*, World Scientific Publishing, 2006.
- [16] S. Mingoo, S. Hanson, D. Sylvester, and D. Blaauw, "Analysis and optimization of sleep modes in subthreshold circuit design," in *Proc. 44th ACM/IEEE Design Automation Conference*, June 2007, pp. 694–699.
- [17] H. T. Friis, "A note on a simple transmission formula," in *Proc. IRE*, 1946, vol. 34, pp. 245–256.
- [18] H. Karl and A. Willig, *Protocols and Architectures for Wireless Sensor Networks*, John Wiley and Sons Inc., first edition, 2005.
- [19] IEEE Standards, "Part 15.4: Wireless Medium Access control (MAC) and Physical Layer (PHY) Specifications for Low-Rate Wireless Personal Area Networks (WPANs)," in *IEEE 802.15.4 Standards*, Sept. 2006.
- [20] L. Barclay, *Propagation of Radiowaves*, The Institution of Electrical Engineers, London, second edition, 2003.
- [21] J. G. Proakis, *Digital Communications*, New York: McGraw-Hill, fourth edition, 2001.
- [22] T. S. Rappaport, *Wireless Communications: Principles and Practice*, Englewood Cliffs, NJ: Prentice-Hall, second edition, 2002.
- [23] R. Min and A. Chadrasakan, "A framework for energy-scalable communication in high-density wireless networks," in *Proc. of International Symposium on Low Power Electronics Design*, 2002.
- [24] IEEE P802.15-09-0329-00-0006, "IEEE P802.15 WG for Wireless Personal Area Networks," May 2009.
- [25] IEEE Standards, "Part 16: Air interface for fixed and mobile broadband wireless access systems," in *IEEE 802.16.e Standards*, 2005.
- [26] A. Shokrollahi, "Raptor codes," *IEEE Trans. on Inform. Theory*, vol. 52, no. 6, pp. 2551–2567, June 2006.
- [27] J. D. Brown, *Adaptive Demodulation Using Rateless Erasure Codes*, Ph.D. Thesis, University of Toronto, 2008.
- [28] T. J. Richardson and R. L. Urbanke, "The capacity of low density parity-check codes under message-passing decoding," *IEEE Trans. on Inform. Theory*, vol. 47, no. 2, pp. 599–618, Feb. 2001.
- [29] "Range extension for IEEE 802.15.4 and ZigBee applications," *FreeScale Semiconductor, Application Note*, Feb. 2007.
- [30] A. Bevilacqua and A. M. Niknejad, "An ultrawideband CMOS low-noise amplifier for 3.1-10.6 GHz wireless receivers," *IEEE Journal of Solid-State Circuits*, vol. 39, no. 12, pp. 2259–2268, Dec. 2004.
- [31] P. Meir, R. A. Rutenbar, and L. R. Carley, "Exploring multiplier architecture and layout for low power," in *Proc. of IEEE Custom Integrated Circuits Conference*, 1996, pp. 513–516.
- [32] O. Etesami and A. Shokrollahi, "Raptor codes on binary memoryless symmetric channels," *IEEE Trans. on Inform. Theory*, vol. 52, no. 5, pp. 2033–2051, May 2006.